



Residual stress distribution of the soldered structure with Kovar alloy and Al₂O₃ ceramics

Qile Gao¹, Jing Wang¹, Yiliang Zhang^{1,*}, Junming Zhou¹, Jiagen Peng², Shouliang Hu², Yanjun Zeng^{3,*}

¹Beijing University of Technology, Beijing 100124, China

²China Academy Of Engineering Physics, Mianyang 621900, China

³Biomechanics and Medical Information Institute, Beijing University of Technology, Beijing 100022, China

Received 7 October 2016; Received in revised 8 November 2016; Received in revised form 24 February 2017;

Accepted 8 March 2017

Abstract

Residual stress distribution in soldered structure of Kovar alloy and Al₂O₃ ceramics was determined using XRD analyses. In order to measure the residual stress, position of the characteristic diffraction peak and stress constant were obtained using several versatile/advanced techniques after calibration. Residual stress of soldered structure was measured based on the diffraction patterns obtained for the distribution of residual stress in the soldered joint. Only diffraction peak at 149° for Kovar alloy and two diffraction peaks ranging from 140–170° for Al₂O₃ ceramics were found to be appropriate for the residual stress determination. It was also confirmed that for Al₂O₃ ceramics the XRD peak at 152° reflects the changes of stress more precisely than the one at 146°. The stress constant K of Kovar alloy and Al₂O₃ ceramics was found to be –197 MPa/° and –654 MPa/°, respectively. After soldering, the maximum residual stress of the soldered joint of both materials developed at 1 mm from the soldering seam, and the values within 3 mm from the soldering seam are generally significant. Thus, it is important to pay attention to the area of 3 mm from the soldering seam in practical application.

Keywords: soldered structure, Kovar alloy and Al₂O₃ ceramics, residual stress distribution, XRD analyses

I. Introduction

At present, ceramic-metal composite structure has been widely used in electronic, space, atomic energy, high-energy physics, energy transportation, machinery, chemical and textile industries [1,2]. The composite structure merges the advantages of their components and adapts well to the needs of modern engineering. One of the most useful materials is Al₂O₃ ceramics-Kovar alloy which combines the properties of both Al₂O₃ ceramics and Kovar alloy. However, as soldering process generates residual stress which directly affects the service life of the structure, it is essential to measure the residual stress [3]. X-ray diffraction (XRD), a mature and non-destructive measurement, is reported to be

an important tool that can measure residual stress. For the feasibility and accuracy of the test, it is necessary to determine the diffraction peak and stress constant of these materials, before studying the residual stress distribution of the soldering joint.

Due to the peculiarity of the ceramic-metal structure, the strength of soldered joint is considered to prevent fracture, especially at the interface of Al₂O₃ ceramic and soldering filler metal [4]. Yu *et al.* [5] studied the joint of Al₂O₃ ceramic and Kovar alloy, and found that a certain thickness of molybdenum attached to the soldering section could avoid cracks. Xin *et al.* [6] revealed that a layer of titanium film plated on the surface of Al₂O₃ would increase the strength of the soldered joint. Fan *et al.* [7], Wang *et al.* [8] and Hattali *et al.* [9] measured the residual stress of the soldered structure with Al₂O₃ ceramics and different materials such as Y-TZP and SiC ceramics. Niu [10] and Zhong [11] also performed relevant experiments on Kovar alloy.

*Corresponding author: tel: +86 010 67391809,

e-mail: zhangyli@bjut.edu.cn (Y. Zhang),

e-mail: yjzeng@bjut.edu.cn (Y. Zeng)

In this study, the residual stress of Al₂O₃ ceramics-Kovar alloy soldered structure was measured. Prior to residual stress measurement, position of the characteristic diffraction peak and stress constant, K , of Al₂O₃ ceramics and Kovar alloy were determined and, thus, the feasibility and accuracy of tests were ensured.

II. Device and method

When crystal structure is affected by residual stress, the lattice plane spacing d will be changed. The basic principle of residual stress determination by XRD analyses is to determine these changes in lattice spacing d , by measuring the changes in diffraction angle 2θ [12], and to calculate the stress values using elastic mechanics methods. The following equation is used to calculate the stress values:

$$\sigma = K \cdot M \quad (1)$$

where K is the stress constant and M indicates the slope of curve 2θ - $\sin 2\psi$ (where ψ is angles between the normal line of diffraction surface and specimen surface).

Residual stress of the soldered structure was measured based on the X-ray diffraction analyses conducted using XRD MSF-2M Rigaku, Japan. Position of the characteristic diffraction peak and stress constant, K , as two important XRD parameters, were determined. As the stress constants of Al₂O₃ ceramics and Kovar alloy were unknown before this study, the stress constant of carbon steel was chosen for the test, and was modified later. By using X-ray diffractometer and uniform strength beam, the theoretical method, electrical test method and X-ray diffraction method were conducted. The selection of appropriate diffraction peak for residual stress determination was also vital for the testing accuracy [13,14]. With these three main methods theoretical stress values, stain gauge stress values and diffraction stress value were measured. Then these values were compared to conclude their characteristics. As the XRD characteristics of Al₂O₃ ceramics and Kovar alloy are the basis of the residual stress research, they were determined first.

2.1. Design of uniform strength beam

The diffraction and strain gauge measurements were conducted on uniform strength beams. Uniform strength beams have the feature that the maximum stress values are same on arbitrary x -section under the load F . By using uniform strength beams, different stress values measured by three methods can be compared and analysed.

When a cantilever beam is subjected to a downward force F at the outer end, the maximum stress σ_{max} on any x -section is:

$$\sigma_{max} = \frac{M_x \cdot y_{max}}{I_z} = \frac{F \cdot x}{W_z} = \frac{6F \cdot x}{b(x) \cdot h^2} \quad (2)$$

where, x is the distance between the loading and measuring point, M_x is the bending moment on x -section,

$M_x(x) = F \cdot x$, W_z is the modulus of the anti-bending section, h and b are the height and width of x -section, respectively. The design width of the uniform strength beam is:

$$b(x) = \frac{6F \cdot x}{h^2 \cdot \sigma_{max}} \quad (3)$$

For uniform strength beams, in order to keep the σ_{max} on any x -section constant, the width b of the beam is proportional to x . Thus, b has the maximum value at the fixed end of the beam. Considering the actual test application that the load F is exerted by suspending the weights at the outer end of the uniform strength beams were transformed into cantilever beams. The experimental model is shown in Fig. 1.

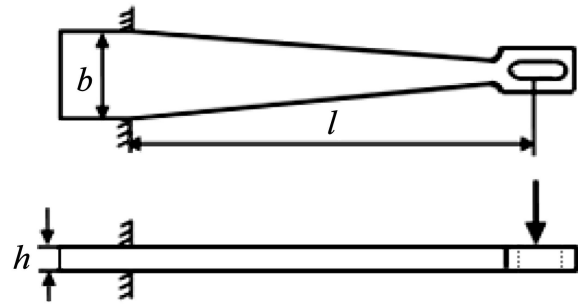


Figure 1. Uniform strength beam

In the test, the dimensions of the Kovar alloy beam were: $h = 6$ mm, $b_{max} = 34$ mm and $l = 300$ mm, whereas the dimensions of Al₂O₃ ceramics beam were: $h = 7$ mm, $b_{max} = 34$ mm and $l = 300$ mm.

2.2. Experimental method

Stress will be produced when a load F is applied on the uniform strength beam. In our experiments three kinds of stress values were measured with three different methods given below, and in order to modify stress constant K , these stress values are compared and analysed.

Theoretical method – According to the characteristics of uniform strength beams, the stress on the beam is calculated using following equation:

$$\sigma = \frac{6F \cdot x}{b \cdot h^2} \quad (4)$$

The stress values calculated by this formula are denoted as theoretical stress values.

Electrical test method – Electrical test method calculates the stress with strain values on the beam. In this study, three strain gauges were pasted along the axis on the surface of the beam as width of beam b is changed with x and the loading point is on the axis. The test results are more accurate by this patching plan. The plan of patching strain gauges is shown in Fig. 2. When the beam was affected by load F and bended, the strain gauges detected the strains of the beam. As every point on the beam was under the uniaxial stressed state, the

stress is calculated by:

$$\sigma = E \cdot \varepsilon_i \quad (5)$$

and the results were the average values of three (n) strain gauges:

$$\sigma = \frac{1}{n} \sum_{i=1}^n E \cdot \varepsilon_i \quad (6)$$

The stress values calculated by this method are denoted as strain gauges stress values.

X-ray diffraction method – By applying the load F step by step, the stress of test points was measured by X-ray stress diffractometer. The Cr- $K\alpha$ and Cu- $K\alpha$ radiations were used for the Kovar alloy and Al_2O_3 , respectively with the following operation parameters: working

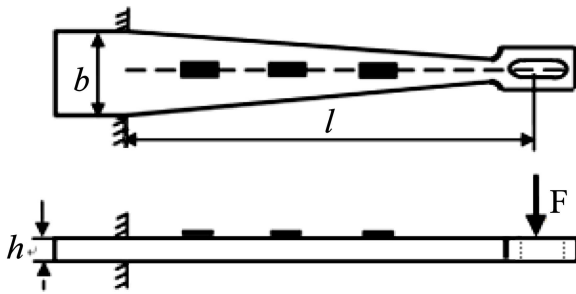


Figure 2. Plan of patching strain gauges

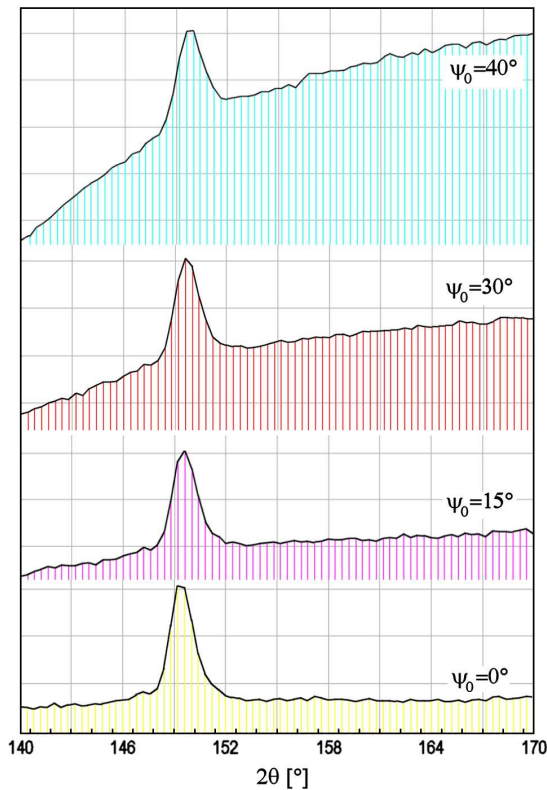


Figure 3. Diffraction spectra of Kovar alloy at different ψ_0 angles (0° , 15° , 30° and 40°)

voltage 30 kV, working current 6–8 mA and ψ_0 angles 0° , 15° , 30° , 40° . The stress values calculated by this measurement are denoted as diffraction stress values.

III. Results and discussion

3.1. Diffraction characteristic of Kovar alloy

At first, Kovar alloy was pre-scanned by X-ray diffractometer. The diffraction spectra of Kovar alloy at different ψ_0 angles are presented in Fig. 3. Then the diffraction data were fitted using seven points smoothing method and processed through Lorentz correction, background correction, and absorption correction. Parabola schemes were used for the diffraction peak characterization. According to Fig. 3, the location of diffraction peak is around 149° .

During experimentation on the uniform strength beams, the theoretical values were calculated by Eq. 4. Electrical test values were obtained using Eq. 6 where elastic modulus was used to be $E = 132$ GPa and the average value of three strain gauges was taken as the test result. The theoretical, electrical test values and diffraction values of uniform strength beams obtained for Kovar alloy are presented in Fig. 4a.

In X-ray diffraction experiments, a constant K_{test} was assumed before the test which was replaced by K of carbon steel. The residual stress values obtained from K_{test} is named σ_{test} . Since K_{test} is different from the K of Kovar alloy, it needed to be modified. As σ_{test} contained two uncertain parts, initial stress σ_0 and systematic error caused by K_{test} , thus, the modification process was divided into two steps.

1. *Eliminating the initial stress σ_0* : Initial stress, σ_0 was developed during manufacturing processes and existed before the experiments. In this test initial stress was -175.5 MPa/ $^\circ$, and the stress was revised as $\sigma_1 = \sigma_{test} - \sigma_0$.

2. *Eliminating the systematic error*: Different slopes between fitted straight line of σ_1 and σ_{true} in Fig. 4 reflect the systematic error caused by K values. According to the X-ray diffraction equation $\sigma = K \cdot M$ where M is the slope of curve $2\theta \cdot \sin 2\psi$. Value of M is independent of both K and σ , and therefore can be expressed as following:

$$M = \frac{\sigma_1}{K_{test}} = \frac{\sigma_{true}}{K_m} \quad (7)$$

and

$$K_m = \frac{\sigma_{true}}{\sigma_1} K_{test} \quad (8)$$

where σ_{true} is the theoretical stress value. Then σ_{true} , σ_1 and K_{test} were substituted into Eq. 7 and K_m was calculated to be -197 MPa/ $^\circ$. The experimental data and modified results were presented in Fig. 4b and showed that revised curve was closed to the curve constructed using theoretical values.

From the diffraction spectra, it is obvious that Ko-

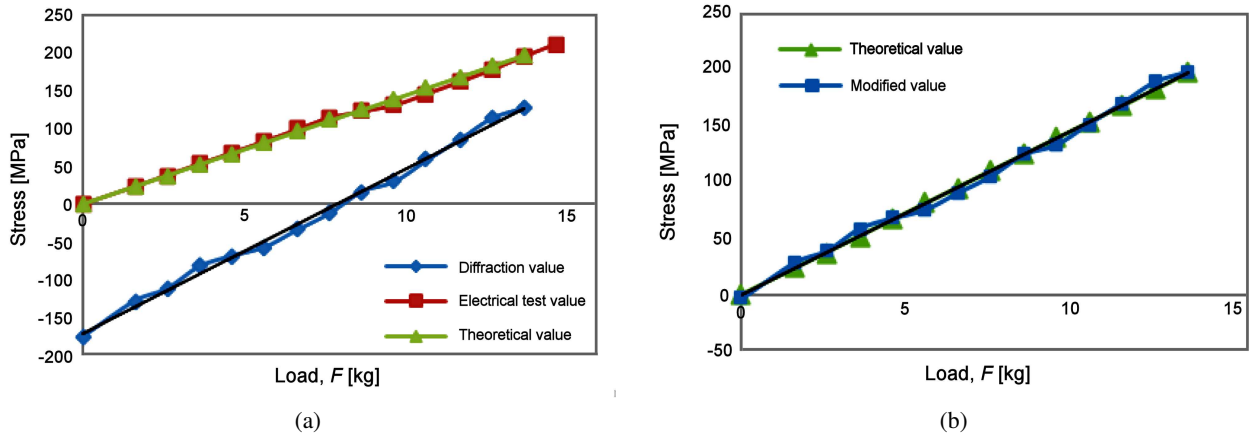


Figure 4. Comparison of diffraction, electrical test and theoretical values (a) and theoretical and modified values (b) for Kovar alloy

var alloy displays only one diffraction peak at around 149° . In addition, the diffraction result based on this peak maintains a linear trend with the applied load F , and after modification, the fitted line was almost consistent with the line constructed by theoretical values.

Finally, through calculation, the K value of Kovar alloy was found to be $-197 \text{ MPa}/^\circ$.

3.2. Diffraction characteristic of Al_2O_3 ceramics

Typical X-ray diffraction patterns of Al_2O_3 ceramics are shown in Fig. 5. From the images, it is clear that there are two obvious peaks in the scanning range and the intensity of the peak at 152° appears to be stronger than of the peak at 146° . As mentioned above, the theoretical values were calculated using Eq. 4 and electrical test values took the average value of three strain gauges at $E = 271 \text{ GPa}$. The comparison of these results is shown in Figs. 6a and 7a. Similar to the modification process of Kovar alloy, the K values of Al_2O_3 ceramics at two diffraction peaks were corrected as follows: for $2\theta = 146^\circ$, $K_{test} = -721.08 \text{ MPa}/^\circ$ and $K_m = -566 \text{ MPa}/^\circ$; and for $2\theta = 152^\circ$, $K_{test} = -696.04 \text{ MPa}/^\circ$ and $K_m = -654 \text{ MPa}/^\circ$. The results after modification are shown in Figs. 6b and 7b. From Fig. 6 it is obvious that Al_2O_3 ceramics displays two diffraction peaks and the strength of diffraction peak at 152° was stronger than the peak at 146° .

The calibrated K value was calculated to be $-566 \text{ MPa}/^\circ$ for XRD peak at 146° . However, the residual stress measured by this peak showed significant fluctuation with changing of the load (Fig. 6), which may be attributed to the smaller scanning angle or impurity peaks interference. Figure 7 manifested that diffraction peak at 152° showed tiny fluctuation and lower test error, meaning better diffraction effects. Residual stress increased with increasing the load, and the fitted curves coincided well with theoretical values. Due to the preferable linear regression relationship and the stable numerical values, it can be suggested that the peak at 152° can be applied in engineering. Finally, the diffrac-

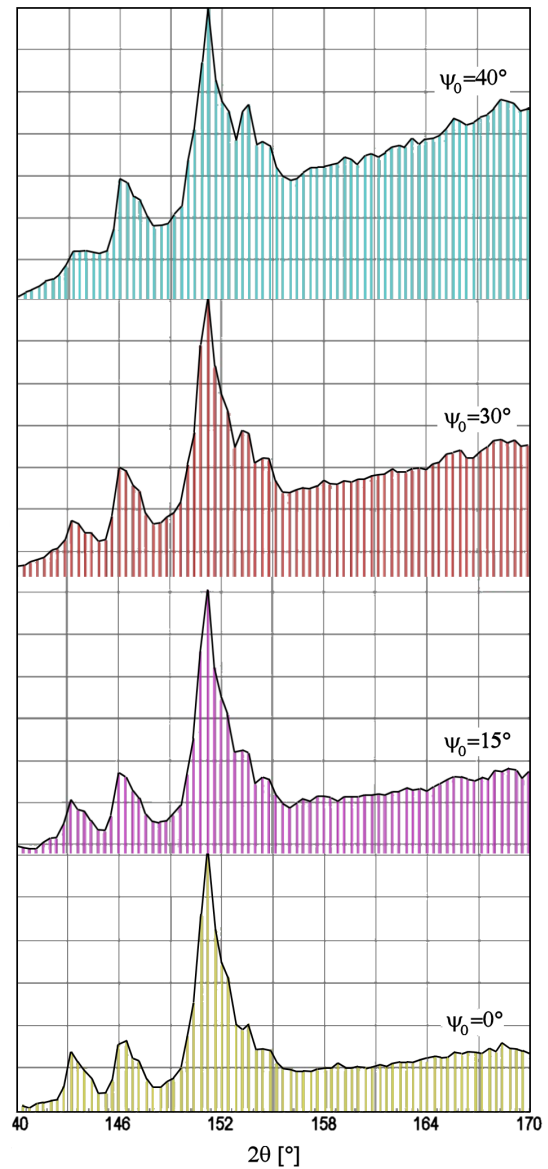


Figure 5. Diffraction spectra of Al_2O_3 ceramics at different ψ_0 angles (0° , 15° , 30° and 40°)

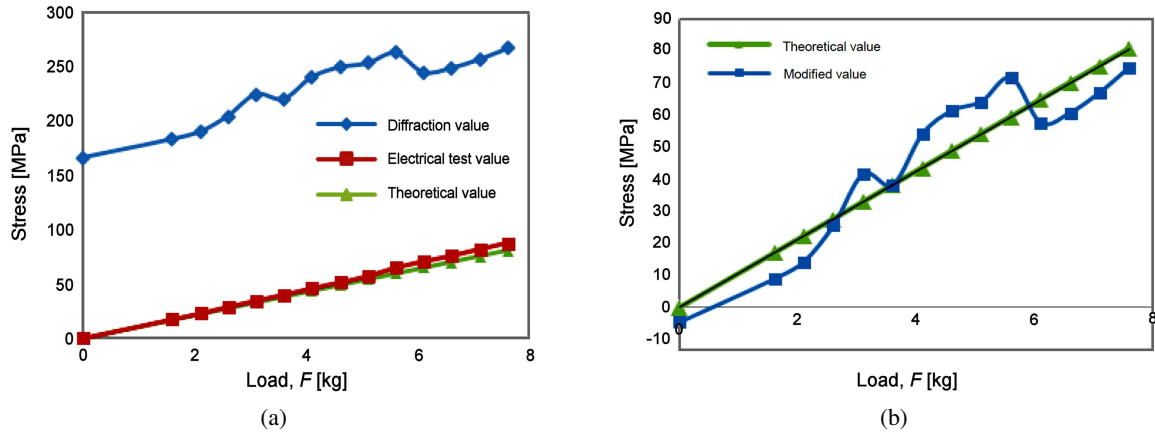


Figure 6. Comparison of diffraction, electrical test and theoretical values (a) and theoretical and modified values (b) for Al_2O_3 ceramics calculated using XRD peak at 146°

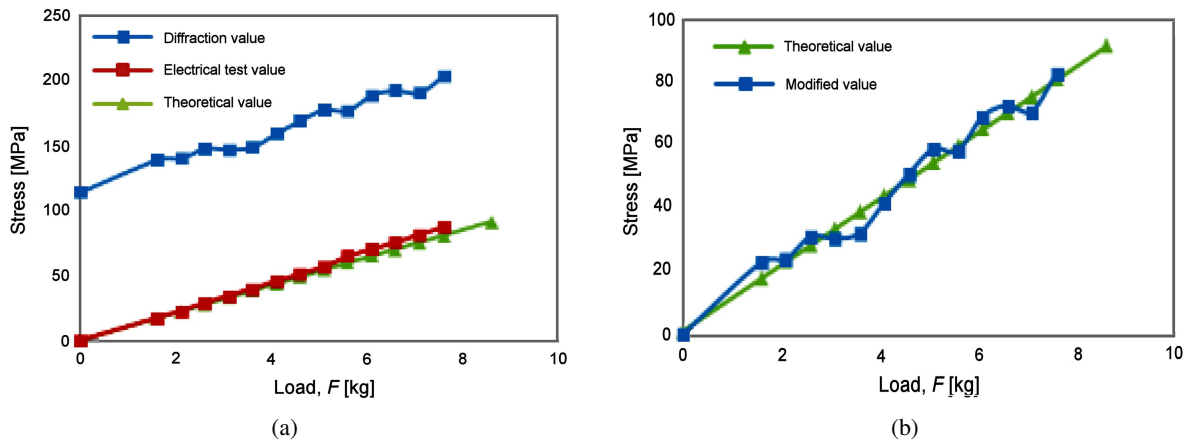


Figure 7. Comparison of diffraction, electrical test and theoretical values (a) and theoretical and modified values (b) for Al_2O_3 ceramics calculated using XRD peak at 152°

tion peak at 152° was selected for Al_2O_3 ceramics and the calibrated stress constant K was calculated to be $-654 \text{ MPa}/^\circ$.

3.3. Characterization of soldered structure

Residual stress test

The soldered joints were adopted amount of Ag and the soldering process was conducted in the hydrogen

soldering furnace under the certain temperature and cooling process. Figure 8 represents the test specimen with 60 mm length, where the length of both ceramics and Kovar alloy is 30 mm. The joint of these two materials is the soldering seam of which the width is 0.2 mm. The test specimen has 3 characteristics: i) the residual stress is uniform along the soldering direction (X axis); ii) the residual stress gradient along the vertical direction (Y axis) is higher; iii) the boundary in-

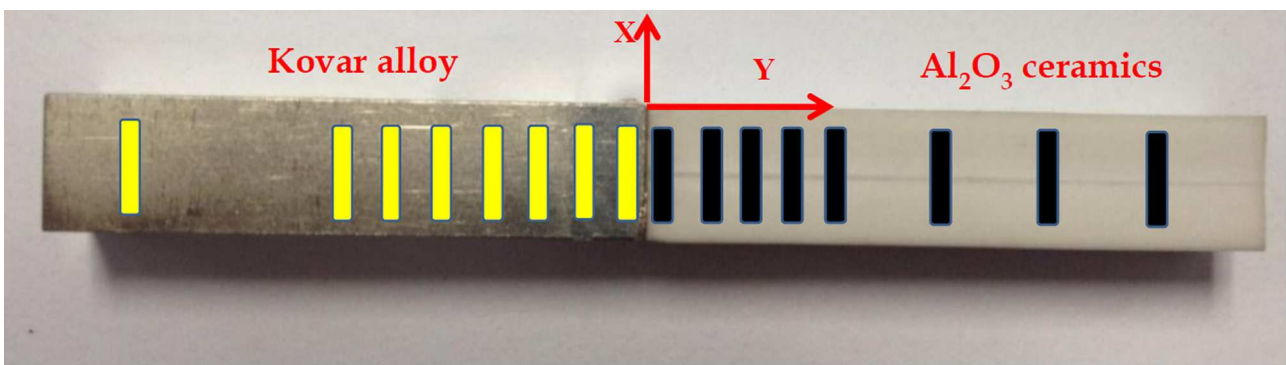


Figure 8. Soldering specimen and measuring points

fluences on stress test. Test area is also shown in Fig. 8. The small yellow rectangles denote the test areas of Kovar alloy, and the black rectangles represent the test areas of Al_2O_3 ceramic. Instead of using the circular test area, the rectangular test area is used, as small and dense test points are required to obtain relatively large diffraction areas. The rectangle shape insures enough diffraction area and reflects stress gradient in the vertical direction.

Experiments in this study were carried out at room temperature. During each test, a rectangular area of 1 mm wide was exposed and other areas were covered using lead sheath. The test was conducted from the soldering joint to the end of the sample, until finishing the last test point.

Residual stress distribution in Kovar alloy

The residual stress distribution of Kovar alloy is displayed in Fig. 9, where the x-axis is the distance between the test point and the soldering seam. The following observations were obtained in Kovar alloy:

1. Residual stress level: Both in parallel (X) and vertical (Y) direction, the highest stress is realized at 1 mm from the soldered joint. The maximum stress in parallel direction was found to be 207.7 MPa, while the maximum stress in vertical direction was -199.5 MPa.

2. Distribution of residual stress: Tensile stress was realized in parallel direction, but compressive stress was developed in vertical direction.

3. The influence of soldering residual stress: The influence range in two directions was 5 mm from the sol-

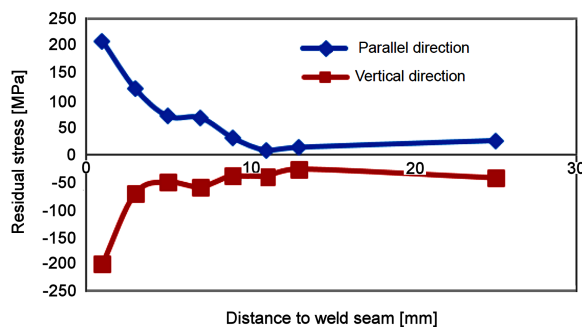


Figure 9. Residual stress distribution in Kovar alloy

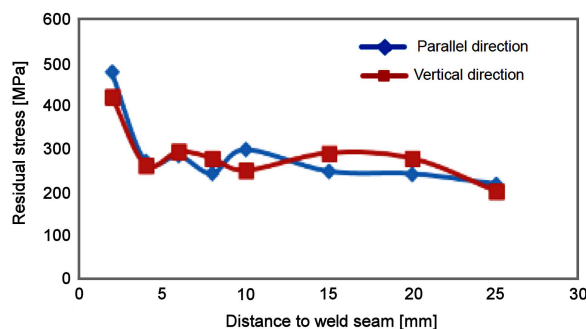


Figure 10. Residual stress distribution in Al_2O_3 ceramics

dered joint, and the residual stress distribution in this range showed a large gradient.

4. The residual stress of the parent material was within ± 50 MPa in both directions.

Residual stress distribution in Al_2O_3 ceramics

Figure 10 represents the residual stress of Al_2O_3 ceramics. Figure 10 shows the characteristics of Al_2O_3 ceramics that:

1. Residual stress level: Both in parallel (X) and vertical (Y) direction, the highest stress is realized at 1 mm from the soldered joint. The maximum stress in parallel direction was 476.4 MPa and the maximum stress in vertical direction was 420 MPa.

2. Distribution of residual stress: Both directions realized tensile stress similar in numerical values. Stress distribution presented “L” state.

3. The influence of soldering residual stress was 3 mm from the soldered joint.

4. The residual stress of the parent material was between 200–300 MPa in both directions.

IV. Conclusions

Residual stress distribution in soldered structure of Kovar alloy and Al_2O_3 ceramics was determined using XRD analyses. It was found that Kovar alloy shows only one diffraction peak at 149° . This diffraction peak maintains a good linear relationship with residual stress and stress constant K . On the other hand, Al_2O_3 ceramics displays two obvious diffraction peaks in the range $140\text{--}170^\circ$. The peak at 146° returns $K = -566$ MPa/ $^\circ$, while the peak at 152° displays $K = -654$ MPa/ $^\circ$. Two diffraction peaks are linearly related to the stress. However, as the peak at 152° reflects the changes in stress more accurately than the peak at 146° , this one was used in tests.

In the Kovar alloy side of the soldered structure, the residual stresses in parallel direction are opposite to vertical direction. While the stress peak value in parallel direction is found to be 208 MPa, its value in vertical direction is about -200 MPa. Further on, soldering influence range is limited within 5 mm. In Al_2O_3 ceramics side, the stress levels are close in both directions, being 476 MPa in parallel direction and 420 MPa in vertical direction. The soldering influence range is limited to 3 mm.

Maximum residual stress in the soldered specimen is located at about 1 mm from the soldering seam which affected the soldering seam and heat affected zone severely. Attention should be paid on the area within 3 mm from the soldering seam and the control of the residual stress in this region has great influence on the strength and life of the component.

References

1. H. Hu, Y. Xu, “The application and market analysis of cermets composites”, *Metal. Funct. Mater.*, **2013** [2] (2013) 36–39.

2. L. Zhang, M. Qin, X. Qu, Y. Lu, X. Zhang, “Active brazing of AlN ceramic with Kovar alloy”, *Vacuum Electronics*, **2009** [4] (2009) 4–7.
3. R.H. Leggatt, “Residual stresses in welded structures”, *Int. J. Pressure Vessels Piping*, **85** [3] (2008) 144–151.
4. M. Rohde, I. Südmeyer, A. Urbanek, M. Torge, “Joining of alumina and steel by a laser supported brazing process”, *Ceram. Int.*, **35** [1] (2009) 333–337.
5. Z. Yu, P. Yang, K. Qi, R. Li, “Effects of Mo interlayer on suppressing cracks in Al₂O₃/Kovar brazed joint”, *Rare Metal Mater. Eng.*, **12** (2008) 2118–2121.
6. C. Xin, W. Liu, N. Li, J. Yan, S. Shi, “Metallization of Al₂O₃ ceramic by magnetron sputtering Ti/Mo bilayer thin films for robust brazing to Kovar alloy”, *Ceram. Int.*, **42** [8] (2016) 9599–9604.
7. K. Fan, J. Ruiz-Hervias, J. Gurauskis, A.J. Sanchez-Herencia, C. Baudin, “Neutron diffraction residual stress analysis of Al₂O₃/Y-TZP ceramic composites”, *Bol. Soc. Esp. Ceram. Vidr.*, **55** [1] (2016) 13–23.
8. H. Wang, L. Gao, J. Guo, “Analysis of the residual stress in Al₂O₃-SiC nanocomposites”, *Sci. China Series E: Technol. Sci.*, **42** [3] (1999) 330–336.
9. M.L. Hattali, N. Mesrati, D. Treheux, “Electric charge trapping, residual stresses and properties of ceramics after metal/ceramics bonding”, *J. Eur. Ceram. Soc.*, **32** [4] (2012) 717–725.
10. J. Niu, J. Lu, Y. Mu, X. Luo, “Brazing of aluminum matrix composites SiC_p/ZL101 to Kovar alloy 4J29”, *Trans. China Welding Institution*, **2010** [5] (2010) 37–40.
11. Z. Zhong, X. Ling, “Analysis of effect factors on residual stresses within glass tube to Kovar alloy brazed joint”, *Chinese Quarterly of Mechanics*, **2011** [2] (2011) 239–243.
12. J. Liu, *Study of X-ray diffraction measurement technology and application to measure residual stress*, M.Sc. thesis, Beijing University of Technology, 2009.
13. T. Kondoh, G. Tokimasa, T. Sasaki, Y. Hirose. “X-ray stress measurement for titanium aluminide intermetallic compound”, *Adv. X-Ray Analysis*, **43** (2000) 107–116.
14. A. Tony Fry, F.A. Kandil, “A study of parameters affecting the quality of residual stress measurements using XRD”, *Mater. Sci. Forum, Residual Stresses VI, ECRS6* (2002) 579–586.